

Simple Method to Synthesize g-C₃N₄ Doped Sn to Reduce Bandgap Energy (E_g)

Chumphol Busabok*, Wasana Khongwong, Piyalak Ngerchuklin

Expert Centre of Innovative Materials, Thailand Institute of Scientific and Technological Research,
35 Mu 3, Khlong Ha, Khlong Luang, Pathum Thani 12120, Thailand

*Corresponding author e-mail: chumphol@tistr.or.th

Received: 21 February 2022 / Revised: 14 March 2022 / Accepted: 14 June 2022

Abstract

Graphitic carbon nitride (g-C₃N₄) has been highlighted in its unique electronic structure with a medium bandgap, high thermal and chemical stability in the ambient environment. It is promoted as a photocatalytic material. To enhance photocatalytic properties, Sn-modified g-C₃N₄ was synthesized from urea and Sn powder. Firstly, urea was fired at 450-650°C in the air to synthesize g-C₃N₄ powder. Then such g-C₃N₄ powder was mixed with Sn powder for 0.1, 0.3, and 0.5 mole ratio and fired at 550°C in ambient. To investigate the phase formation and light absorption, XRD and light absorption spectrophotometers were performed, respectively. The light absorption value was used to calculate band gap energy (E_g). It was found that the XRD results of synthesized g-C₃N₄ were on the broad peak to narrow peak in synthesized temperatures 450-650°C. The light absorption of synthesized powder at 550°C was higher than others. Thus, synthesized powder at 550°C was chosen to mix with Sn powder. It observed that E_g of Sn-modified g-C₃N₄ decreased depending on the amount of Sn and synthesized temperatures.

Keywords: Graphitic carbon nitride, Bandgap energy, Light absorption

1. Introduction

Graphitic carbon nitride (g-C₃N₄) is a metal-free and conjugated polymeric with a formula of (C₃N₃H)_n in which covalent C-N bonds called tri-s-triazine unit connected with planar amino acid groups in the layer and hold together with van der Waals forces. This structure makes it excellent in thermal and chemical stability and stable allotrope (Kong et al., 2021). It possesses an electronic structure with a narrow bandgap (2.7 eV) and is responsible for visible light photocatalyst at 400-450 nm (Song et al., 2019). Since then, g-C₃N₄ has much attention in many applications including organic pollutants, remediation environment (Alulema-Pullupaxi et al., 2021), hydrogen evolution (Naseri, Samadi, Pourjavadi, Moshfegh, & Ramakrishna, 2017) and fuel cell (Zheng, Liu, Liang, Jaroniec, & Qiao, 2012), water spitting (Neelakanta Reddy et al., 2021) and antibacterial activity (Huang, Ho, & Wang, 2014; Neelakanta Reddy et al., 2021).

However, pristine g-C₃N₄ shows less efficiency due to low surface area resulting in a low active site, high charge recombination rate and small harvest of solar energy (Wen, Xie, Chen, & Li, 2017). So, to obtain high photocatalytic activities, tailoring and customizing of the structures by doping with metallic (Shanmugam, Muppudathi, Jayavel, & Jeyaperumal, 2020; Van et al., 2022) and/or non-metallic elements (Li et al., 2014), and hybridization (Zhang, Yu, Sun, & Zheng, 2018) have been performed. Some researchers applied some solutions by reducing E_g with S-scheme heterojunctions (Van Viet et al., 2021). Therefore, the aim of this research was to study the effect of metallic Sn powder doped in g-C₃N₄ to reduce band gap energy (E_g). The mixing and calcination of urea and Sn powder were performed at 550°C in air atmospheric by tube furnace. The observation of synthesized g-C₃N₄ and Sn-doped g-C₃N₄ powders including phase analysis, crystal size, light absorption together with

photocatalytic efficiency such as calculated E_g and degradation of methylene blue were performed and discussed.

2. Materials and Methods

2.1 Synthesis of g-C₃N₄

The g-C₃N₄ powder was prepared by the simple method, the 20 g of urea powder was used as a precursor and placed in an alumina crucible and followed by heated up in a tube furnace at 400°C-650°C with the interval of 50°C in air atmosphere for 0.5, 2 and 3 h. The synthesized powders were characterized by XRD (1.54 Å Cu, Shimadzu XRD6000). The crystal size was calculated from the main peak of g-C₃N₄ by measuring full-width half maximum (FWHM) and calculated by Scherrer's equation (1).

$$D = K\lambda/\beta\cos\theta \quad (1)$$

Where $K = 1$

D is crystal size

λ is the wavelength of the x-ray

β is FWHM

θ is diffraction angle

The light absorption of synthesized powder was measured by UV-Vis-NIR spectrophotometer (ES Avalight-DHS; Detector AvaSpec-2048L; UV/Vis/NIR range from 200 to 2500 nm). And band gap energies (E_g) of the synthesized powders were calculated from light absorption data as followed (2):

$$E_g (\text{eV}) = hc/\lambda = 1239.8/\lambda \quad (2)$$

Where h is Planck's constant

c is speed of light

λ is cut off wavelength

2.2 Synthesis of g-C₃N₄ doped Sn

For the Sn doping, the g-C₃N₄ powder with the best light absorption from 2.1 was doped with Sn powder for 0.1, 0.3 and 0.5 % by mole. The two materials were continued dry mixing and heated up at 550°C in an air atmosphere for 0.5 h in an alumina

crucible. The obtained Sn-doped g-C₃N₄ were examined phase, light absorption and calculated band gap energies (E_g) as the same equipment in section 2.1.

2.3 Methylene blue degradation testing

For methylene blue degradation testing, 50 mg of g-C₃N₄ or Sn doped g-C₃N₄ were dispersed in 5 ppm of methylene blue solution (50 ml.) and illuminated by 50 watts, 110 Ln/watt LED lamp for 1-12 hrs. The light absorption of methylene blue was measured by UV-Vis-NIR spectrophotometer to observe the degradation rate of methylene blue from decreasing concentration. The formula of the degradation was calculated as followed (3):

$$\text{Degradation (\%)} = [(C_0 - C)/C_0] \times 100\% \quad (3)$$

Where C_0 is the initial concentration of methylene blue

C is the concentration at a time t .

3. Results and Discussions

3.1 The effect of synthesized temperature on phase and light absorption of g-C₃N₄

The results of phase analysis, crystal size and light absorption by XRD and UV-Vis-NIR, respectively, of the obtained g-C₃N₄ powders at 400°C-650°C in the air atmosphere were demonstrated. XRD graph (Figure 1) showed that urea (CH₂N₂O) was gradually decomposed to ammeline (C₃H₅N₃O) at 400°C and completely changed at 450°C. After heating up to 500°C and higher, ammeline was transformed to g-C₃N₄ phase according to JCPDS card number of 75-0454. The highest peak of XRD at 2θ of 27.8 was used to calculate crystal size by Full width-half max (FWHM) and equation (1). The obtained crystal size of g-C₃N₄ was increased by increasing temperature (Figure 2). However, the oxidation reaction occurred at 550°C and higher, resulting in a small amount of g-C₃N₄ being yielded. The light absorptions of g-C₃N₄ at various synthesized temperatures (Figure 3) were not significantly different and all calculated

E_g of powders were approximately 2.82 eV. However, E_g of g-C₃N₄ at 550°C was a little higher than other synthesized temperatures. Thus, such powder at 550°C was used to study for tin-doped g-C₃N₄ in the further experiment.

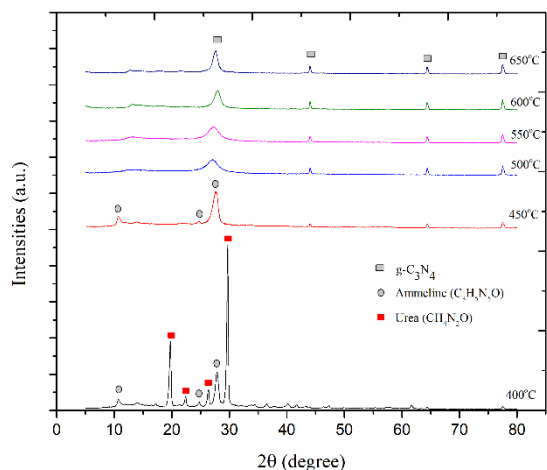


Figure 1. XRD patterns of the g-C₃N₄ powders calcined at temperatures of 400-650°C.

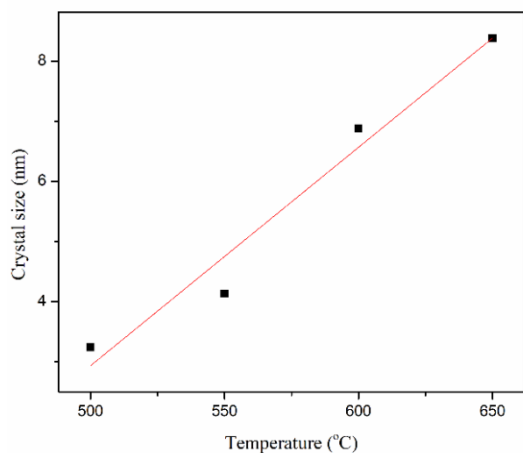


Figure 2. The relationship of g-C₃N₄ crystal sizes to calcination temperatures.

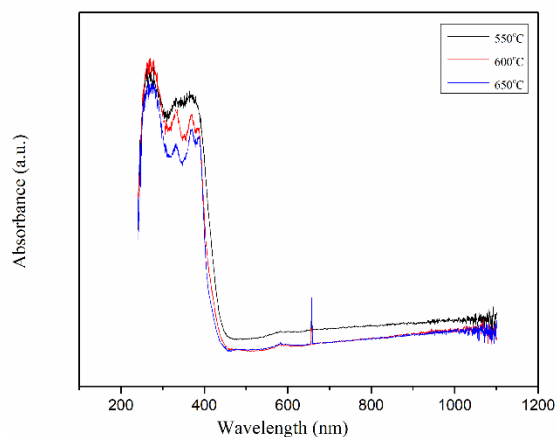


Figure 3. Light absorbance of g-C₃N₄ powders at different calcination temperatures.

3.2 The effect of soaking time on phase and light absorption of g-C₃N₄

From the previous section, the g-C₃N₄ powder calcined at 550°C in the air atmosphere was chosen to study the effect of soaking time for 0.5, 2 and 3 hrs. The results of phase analysis, crystal size and light absorptions were shown in Figures 4-6, respectively. All samples showed absolutely g-C₃N₄ phase (Figure 4) without any residue precursor. The crystal size of the obtained g-C₃N₄ powders were increased when longer soaking time proceeded. The crystal size of 0.5, 2 and 3 hrs soaking was about 4.01, 4.32 and 6.75 nm, respectively (Figure 5). The light absorptions at various soaking times (0.5 and 3 hrs) (Figure 6) were not significantly different and calculated E_g were approximately 2.63 eV. Thus, the least soaking time of 0.5 h was used to study for tin-doped g-C₃N₄ in the further experiment.

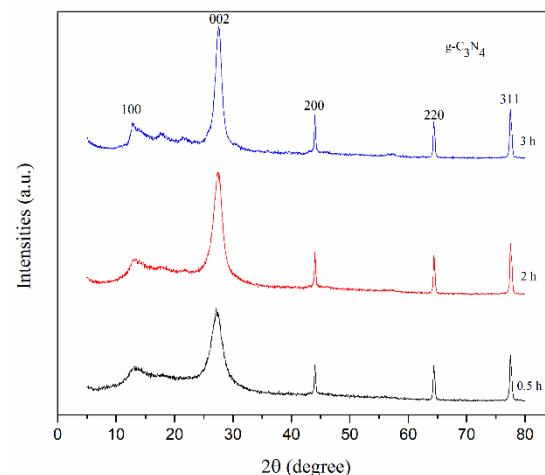


Figure 4. XRD patterns of the g-C₃N₄ powder at various soaking times.

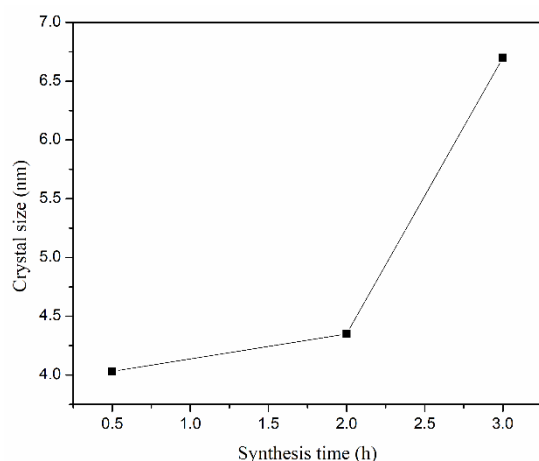


Figure 5. The relationship of $g\text{-C}_3\text{N}_4$ crystal size to the soaking time.

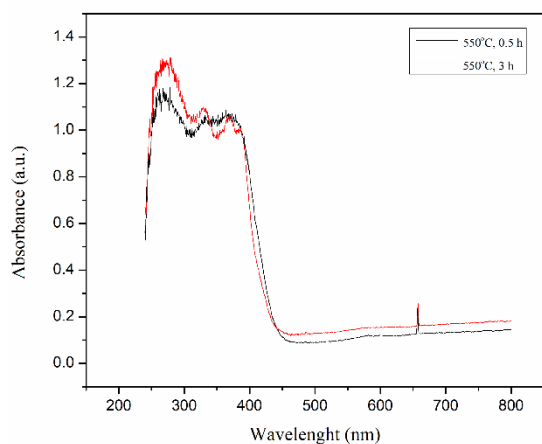


Figure 6. Light absorbance of $g\text{-C}_3\text{N}_4$ powder at various soaking times

3.3 The effect of Sn doped $g\text{-C}_3\text{N}_4$ on phase and light absorption

The $g\text{-C}_3\text{N}_4$ powder synthesized at temperature 550°C for 0.5 h. was doped with metallic Sn powder at 0.1, 0.3 and 0.5 mole percent, dry mixing and then heated up again at 550°C for 0.5 h in the air atmosphere. The results of phase analysis light absorption and calculated E_g were shown in Figures 7-10. Figure 7, XRD graph showed less crystalline $g\text{-C}_3\text{N}_4$ phase due to Sn substituted in the carbon position of the $g\text{-C}_3\text{N}_4$ structure. The more doping content, the higher the amorphous phase was obtained. The limitation of Sn doped was about 0.5 % by mole because some Sn was oxidized to form SnO_2 and so at this Sn content, $g\text{-C}_3\text{N}_4$ changed the

structure. This could be observed by no sharp peak as found in Figure 4. The light absorption from the end of the ultraviolet to visible light range (280-400 nm) was increased in Figure 8. Moreover, light absorption had trended to higher by increasing the amount of Sn dopant. The calculated E_g (Figures 9 and 10) was reduced from 2.82 ($g\text{-C}_3\text{N}_4$) to 1.98 eV (doped 0.5 % mole Sn $g\text{-C}_3\text{N}_4$). The cause of decreasing in E_g can be predicted in two ways, first, when Sn was oxidized, it became SnO_2 , which led to electron transfer from $g\text{-C}_3\text{N}_4$ to SnO_2 at interface heterojunction until the electric potential of Fermi level would be the same (Van et al., 2022). This phenomenon exhausts the electron region on $g\text{-C}_3\text{N}_4$ and electron deposition layer on SnO_2 resulting in an internal electric field (IEF) directed from $g\text{-C}_3\text{N}_4$ to SnO_2 . Second, Sn had substituted to the C-position in $g\text{-C}_3\text{N}_4$ structure, resulting in increased electrical conductivity and change in color to near red. Therefore, it could absorb visible light at an extended wavelength. In this case, there was a high probability that the two above possibilities could occur. The effect of Sn on altered properties of $g\text{-C}_3\text{N}_4$ was increasing the absorption of the visible light from 450 to 650 nm., covering to yellow, making it able to absorb light from the natural source (Solar) or LED lamps with the highest intensities in the blue to yellow as shown in Figure 11. The high light absorption of photocatalytic materials allows them to be better activated to the photocatalytic mechanism which the results of the experiment in section 3.4 can confirm this statement.

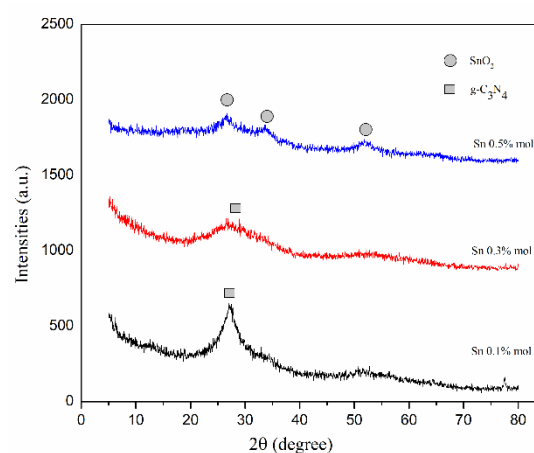


Figure 7. XRD patterns of the g-C₃N₄ powder with various amounts of Sn doping.

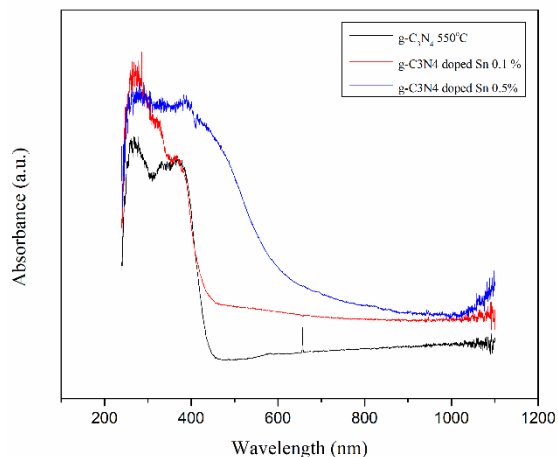


Figure 8. Light absorbance of g-C₃N₄ powder with various amounts of Sn doping.

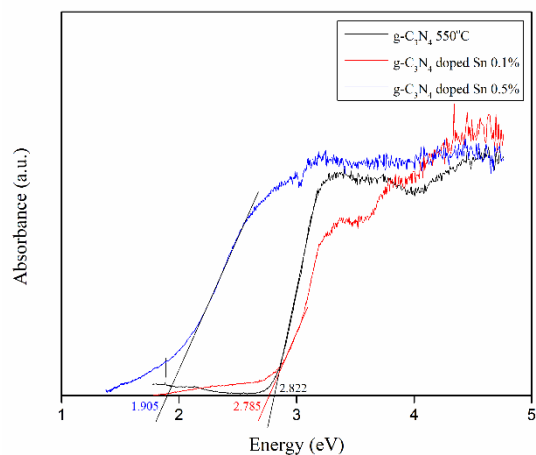


Figure 9. bandgaps of g-C₃N₄ with difference doped Sn.

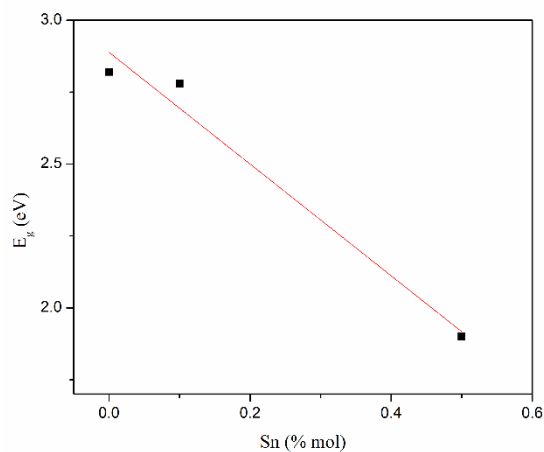


Figure 10. E_g of Sn doped g-C₃N₄ powders

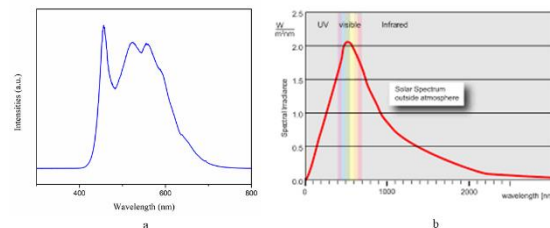


Figure 11. Light source spectrum (a) LED spectrum and (b) solar spectrum.

3.4 Methylene blue degradation testing results

The results of methylene blue degradation testing of g-C₃N₄ and 0.5 Sn-doped g-C₃N₄ were shown in Figures 12-14 and 15-17, respectively. By using visible light 500-700 nm to expose photocatalytic materials, it was found that the g-C₃N₄ absorbed more light when longer time radiation was exposed resulting in higher degradation of methylene blue. At the 12th h, methylene blue was completely clear color. While degradation 0.5 Sn-doped g-C₃N₄ was complete at the 8th h of light irradiation. From the two experiments, it could conclude that photocatalytic performance of 0.5 % mol Sn-doped g-C₃N₄ was more effective than g-C₃N₄ and its reaction was faster than that of g-C₃N₄ about 2.45 times.

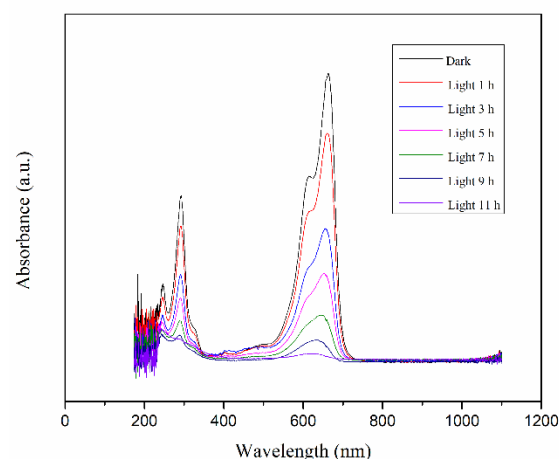


Figure 12. The light absorption of g-C₃N₄

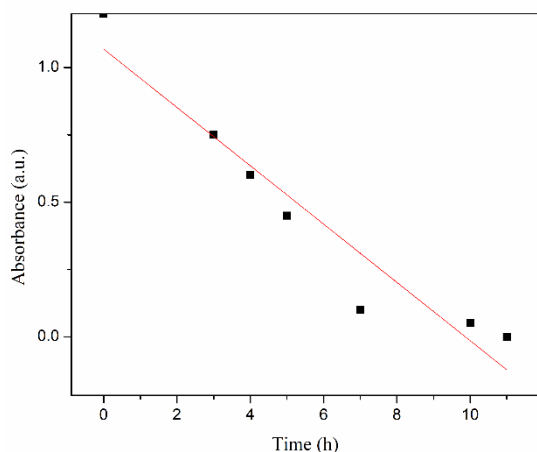


Figure 13. The light absorption at various times of $g\text{-C}_3\text{N}_4$

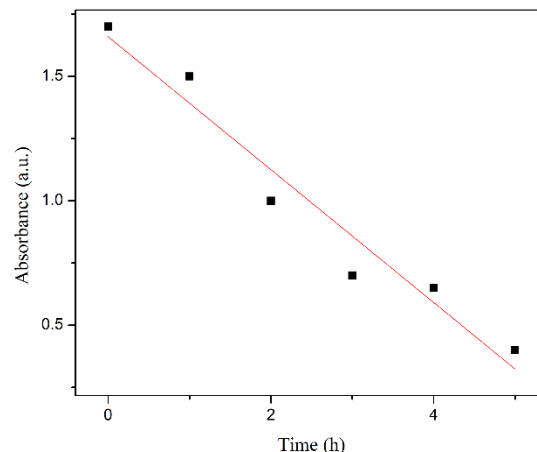


Figure 16. The light absorption at various times of Sn-doped $g\text{-C}_3\text{N}_4$.



Figure 14. The degradation of MB of $g\text{-C}_3\text{N}_4$.



Figure 17. The degradation of MB of Sn-doped $g\text{-C}_3\text{N}_4$.

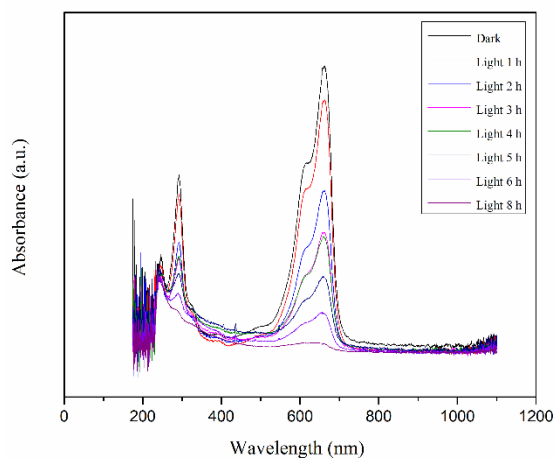


Figure 15. The light absorption of Sn-doped $g\text{-C}_3\text{N}_4$.

4. Conclusions

Sn-modified $g\text{-C}_3\text{N}_4$ was synthesized from urea and metallic Sn powder. Firstly, urea was calcined at $450\text{-}650^\circ\text{C}$ in the air atmosphere to synthesize $g\text{-C}_3\text{N}_4$ powder. Then such $g\text{-C}_3\text{N}_4$ powder was mixed with Sn powder for 0.1, 0.3, and 0.5 mole percent and fired at 550°C in ambient. The conclusion could be drawn as follow:

1. Sn was substituted in $g\text{-C}_3\text{N}_4$ structure and showed the high absorption of violet-blue and green colors to excite the photocatalytic activity.
2. E_g could obviously be reduced by 0.5 % mol Sn-doped $g\text{-C}_3\text{N}_4$.
3. E_g down from 2.82 ($g\text{-C}_3\text{N}_4$) to 1.98 eV. (0.5 % mol Sn-doped $g\text{-C}_3\text{N}_4$) which could reflect in the yellow light range.
4. The 0.5 % mol Sn-doped $g\text{-C}_3\text{N}_4$ could degrade methylene blue faster than $g\text{-C}_3\text{N}_4$ about 2.45 times.

5. Acknowledgement

This work was partially funded by the National Research Council of Thailand (NRCT), the section of PM 2.5, in the project: Development of silicon carbide air filters from cellulose coated with photocatalyst, 2020.

6. References

- Alulema-Pullupaxi, P., Espinoza-Montero, P. J., Sigcha-Pallo, C., Vargas, R., Fernandez, L., Peralta-Hernandez, J. M., & Paz, J. L. (2021). Fundamentals and applications of photoelectrocatalysis as an efficient process to remove pollutants from water: A review. *Chemosphere*, 281, 130821. doi:10.1016/j.chemosphere.2021.130821
- Huang, J., Ho, W., & Wang, X. (2014). Metal-free disinfection effects induced by graphitic carbon nitride polymers under visible light illumination. *Chemical Communications*, 50(33), 4338-4340. doi:10.1039/C3CC48374F
- Kong, X., Liu, X., Zheng, Y., Chu, P. K., Zhang, Y., & Wu, S. (2021). Graphitic carbon nitride-based materials for photocatalytic antibacterial application. *Materials Science and Engineering: R: Reports*, 145, 100610. doi:10.1016/j.mser.2021.100610
- Li, Y., Wu, S., Huang, L., Wang, J., Xu, H., & Li, H. (2014). Synthesis of carbon-doped g-C₃N₄ composites with enhanced visible-light photocatalytic activity. *Materials Letters*, 137, 281-284. doi:10.1016/j.matlet.2014.08.142
- Naseri, A., Samadi, M., Pourjavadi, A., Moshfegh, A. Z., & Ramakrishna, S. (2017). Graphitic carbon nitride (g-C₃N₄)-based photocatalysts for solar hydrogen generation: Recent advances and future development directions. *Journal of Materials Chemistry*, 5, 23406-23433. doi:10.1039/C7TA05131J
- Neelakanta Reddy, I., Veeranjanya Reddy, L., Jayashree, N., Venkata Reddy, Ch., Cho, M., Kim, D., & Shim, J. (2021). Vanadium-doped graphitic carbon nitride for multifunctional applications: Photoelectrochemical water splitting and antibacterial activities. *Chemosphere*, 264, 128593. doi:10.1016/j.chemosphere.2020.128593
- Shanmugam, V., Muppudathi, A. L., Jayavel, S., & Jeyaperumal, K. S. (2020). Construction of high efficient g-C₃N₄ nanosheets combined with Bi₂MoO₆-Ag photocatalysts for visible-light-driven photocatalytic activity and inactivation of bacterias. *Arabian Journal of Chemistry*, 13(1), 2439-2455. doi:10.1016/j.arabj.2018.05.009
- Song, Y., Gu, J., Xia, K., Yi, J., Chen, H., She, X., ... Xu, H. (2019). Construction of 2D SnS₂/g-C₃N₄ Z-scheme composite with superior visible-light photocatalytic performance. *Apply Surface Science*, 467-468, 56-64. doi:10.1016/j.apsusc.2018.10.118
- Van, K. N., Huu, H. T., Nguyen Thi, V. N., Le Thi T. L., Truong, D. H., Truong, T. T., ... Vasseghian, Y. (2022). Facile construction of S-scheme SnO₂/g-C₃N₄ photocatalyst for improved photoactivity. *Chemosphere*, 289, 133120. doi:10.1016/j.chemosphere.2021.133120
- Van Viet, P., Nguyen, H.-P., Tran, H.-H., Bui, D.-P., Hai, L. V., Pham, M.-T., ... Thi, C. M. (2021). Constructing g-C₃N₄/SnO₂ S-scheme heterojunctions for efficient photocatalytic NO removal and low NO₂ generation. *Journal of Science: Advanced Materials and Devices*, 6(4), 551-559. doi:10.1016/j.jsamd.2021.07.005
- Wen, J., Xie, J., Chen, X., & Li, X. (2017). A review on g-C₃N₄-based photocatalysts. *Apply Surface Science*, 391(Pt B), 72-123. doi:10.1016/J.APSUSC.2016.07.030
- Zhang, W., Yu, C., Sun, Z., & Zheng, S. (2018). Visible-light-driven catalytic disinfection of Staphylococcus aureus using sandwich structure g-C₃N₄/ZnO/stellerite hybrid photocatalyst. *Journal of Microbiology and Biotechnology*, 28(6), 957-967. doi:10.4014/jmb.1712.12057

Zheng, Y., Liu, J., Liang, J., Jaroniec, M., & Qiao, S.

(2012). Graphitic carbon nitride materials: Controllable synthesis and applications in fuel cells and photocatalysis. *Energy & Environmental Science*, 5(5), 6717-6731.

doi:10.1039/C2EE03479D